Development of a Low-Cost Stationary Laser Scanning System for Generation of Building Information Models

Syed Riaz un Nabi Jafri[1, *], Muhammad Owais Ali Siddiqui[1], Faraz Akbar[2], Abdul Basit[1], Sheraz Shamim[1], Saad Ahmed[1]

[1]*Department of Electronic Engineering, NED University of Engineering and Technology, University Road, Karachi, Pakistan*

[2]*Department of Automotive and Marine Engineering, NED University of Engineering and Technology, University Road, Karachi, Pakistan*

riazun1036@neduet.edu.pk

***Abstract*—This paper presents a method for developing a 3D point cloud map of any indoor and outdoor vicinities using an indigenously developed stationary scanning system comprising of a single low cost 2D laser scanner. The data logging of scanner and required inertial measurement units (IMUs) has been carried out using a Robot Operating System (ROS). Multiple divergent environments have been scanned and 3D point clouds have been developed, which have been found accurate when compared to the ground truth. In addition, the Building Information Model (BIM) of the surveyed vicinities have been developed using generated point clouds. Compared to available surveying solutions present in the local market, the developed system has been found accurate, faster, economical, and user-friendly to generate structural results of the surveyed vicinities in detail.**

***Index Terms*—Sensor fusion; 3D point cloud; 2D laser scanner; BIM; IMU.**

I. INTRODUCTION

Digital surveying applications that use recent laser scanning technology have been progressively growing around the world. Many scanning systems are in use for indoor and outdoor surveying tasks to build structural models of visited entities and their surroundings. Information gathered during inspection and modelling of under construction or fully furnished buildings is considered very significant for various applications [1]. Different multi-range laser scanners are commercially available in the market with various technical specifications in terms of weight, size, and scanning capacity such as 2D Hokuyo and 3D Velodyne laser scanners. There are many methods in use to collect scanned point cloud data from indoor and outdoor environments, such as using the Simultaneous Localization and Mapping (SLAM) technique applied on backpack or moving trolley systems [2]. The backpack or hand-held systems are often used for various applications [3]. The performances of two portable mobile mapping systems have been presented, including the hand-held ZEB-REVO and the Leica Pegasus backpack systems in indoor and outdoor regions [4]. On the other hand, compact terrestrial or stationary laser scanning systems are in use in many disciplines of engineering, including architecture, archaeology, and surveying tasks [5]. A modern rotating mechanism-based scanning system design has been presented by researchers to build the 3D model using multi-beam scanners [6]. These kinds of systems have been developed to specifically scan the targeted vicinity from the desired perspective. If structural aspect of a targeted wall is desired, then these systems are ideal for only providing scan of such a region. The reported system generates the 3D point cloud by observing the rotation rates of 2D single- or multi-layer scanners. A group of researchers has presented the same rotating mechanism interfaced with a moving platform to generate the 3D point cloud [7].

This paper presents designing and working of a custom made stationary scanning system in various environments using only a single low-cost 2D Hokuyo laser scanner as shown in Fig. 1. A compact two degree of freedom platform has been fabricated to mount the scanner on top along with three HD cameras for performing surveying applications and to build 3D point cloud map. Moreover, the developed point cloud has been used to build information models and floor plans as required by surveyors and civil contractors.

Fig. 1. Applications of the stationary scanning system in various environments.

The rest of the paper is organized as follows. Section II

Manuscript received 25 June, 2022; accepted 3 September, 2022.

This research is supported by the Higher Education Commission (HEC), Pakistan under Grant No. NRPU-6061.

narrates briefly related references and research works. In Section III, the mechanical design and instrumentation scheme are presented. Section IV describes the methodology adopted to generate 3D mapping and point cloud generation along with establishing building information model (BIM) of surveyed regions. In Section V, results of performed tests are explained. In the last section, conclusions and acknowledgment statements are presented.

II. Related Works

The compact and single scanning device-based surveying and mapping systems have been designed mainly using three techniques, which are hand-held single-layer scanning systems, terrestrial systems with multi-layer scanner, and stationary scanning systems with motorised single-layer scanner. These systems are widely used for various applications such as building construction monitoring, industrial surveys, and indoor vicinity mapping. Handheld mobile terrestrial laser scanning (HMTLS) provides high mobility, limited operational cost, and reduced data collection time due to lightweight, rugged, and simple to use design. Multiple products from ZEB are available in the market, both 2D and 3D, according to range, accuracy, and application demand as shown in Fig. 2. One of the products is ZEB Go which is lightweight and easy to process, as summarised in Table I [8]. Another product is ZEB Revo RT which is capable of generating highly accurate 3D models [9]. ZEB Horizon is a high-end hand-held product from ZEB that provides a range of 100 m for indoor, outdoor, and underground digital mapping [10]. These systems are also being used in close-range sensing and large-scale monitoring of forest dynamics and related plantation studies [11].

(a) (b) (c)

Fig. 2. Hand-held laser scanners: (a) ZEB Go, (b) ZEB Revo RT, and (c) ZEB Horizon.

TABLE I. COMPARISON OF MULTIPLE LASER SCANNING SYSTEMS.

Product category	Type of laser scanners	Other Sensors	Max Range	Motorised Joints
ZEB GO	2D	IMU	30 m	-
ZEB REVO RT	2D	IMU Camera	30 m	-
ZEB Horizon	3D	Camera	100 m	1
Leica HDS 7000	3D	-	180 m	1
FARO Focus 70	3D	Camera GPS	70 m	1

The Terrestrial laser scanners (TLS) are relatively expensive; however, their spatial accuracy is very high. Data collection requires careful planning, which is really quite difficult in indoor spaces where visibility is limited due to pillars and walls. They have been used in surveying the ground profile of high-speed roads where traditional surveying is difficult to carry out without road closure [12]. A popular and survey-grade accurate Leica HDS 7000 ultra high-speed laser scanner is in use for different applications as shown in Fig. 3 [13]. Leica HDS 7000 is a versatile, multi-purpose 3D laser scanner that combines high efficiency with high accuracy for a broad range of civil engineering, plant, and building projects. Another popular product, the FARO Focus S70 ultra-portable laser scanner captures ultra-high accurate measurements of objects and buildings with speed and ease [14]. RIEGL VZ-2000i provides high accuracy and range for multiple target objects with an integrated GNSS receiver and offers greater flexibility and interfacing support for a highly accurate geo-referenced solution [15]. However, the majority of these TLS systems are too expensive and complex to train small business enterprises which need low-cost and easy-to-use systems.

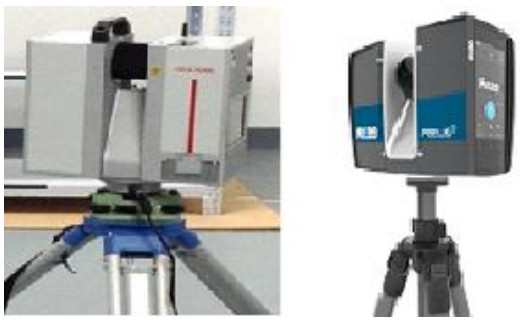

(a) (b)

Fig. 3. Terrestrial laser scanners: (a) Leica HDS7000, (b) FARO Focus.

On the other hand, combining 2D laser scanners with motorised platforms provides a compromised 3D scanning system at economical rates. Similar work has been presented by researchers in [16]. They mounted the SICK 2D laser scanner on a rotational base to construct the 3D laser scanner system. A group of researchers have designed and developed a real-time and low-cost 3D perception and reconstruction system [17]. The 3D mapping system is based on a rotating 2D Hokuyo 30LX laser scanner, driven by a stepper motor, which is suitable for both autonomous navigation and large-scale vicinity reconstruction. In [18], authors presented a servo controlled gimbal to rotate the URG-04LX laser scanner and to extrapolate the 2D data to a 3D sphere. In [19], researchers have demonstrated a similar design scheme by mounting a commercial 2D SICK LMS291 laser scanner on a three-dimensional spinning platform and the 3D motions in the environment have been evaluated using the system.

III. Design of a Stationary Scanning System

A. Mechanical Design

To develop mechanical structure of the desired motorised platform hardware for indoor and outdoor stationary

surveying applications, the mechanical CAD model of the platform has initially been designed in the SolidWorks software as shown in Fig. 4. The main base platform comprising a rectangular box is used for installation of a vertically mounted motor coupled with rotating plate. The motor joint has been designed to rotate ±90 ° to provide required views to the scanning system. A potentiometric encoder along with IMU have been associated with the rotating plate. This plate serves as the housing of the upper structure. Two pillars have been installed on the plate to integrate a top square box platform connected to a second horizontally coupled motor. The second motor joint has been designed to rotate ±90 ° to provide required rotation to view the surveying region. Another potentiometric encoder along with the second IMU have been associated with the rotating top platform. On the top platform, a 2D Hokuyo laser scanner has been mounted along with three HD cameras in the left, right and center positions. The main base rectangular box platform is also used to place the required electronic components and batteries for the stationary system. The bottom surface of the rectangular box has sufficient provision to place the complete structure on a tripod or on a flat surface.

After finishing the CAD model, manufacturing of the motorised stationary scanning system has been initiated. The complete structure is manufactured with 0.5 cm thick acrylic sheet to provide good strength at lightweight as shown in Fig. 5. To get precision in the system, the acrylic sheet has been cut using laser cutting machine to keep minimal tolerance in the actual system. For rotating applications, hybrid stepper motors (NEMA 17) have been installed in the system. These motors provide good precision at high torque and are generally used in CNC machines. Two IMUs (MPU 6050) have been installed in the system along with encoders to perceive rotational changes. Finally, Hokuyo UTM-30LX laser scanner and cameras have been installed as shown in Fig. 5.

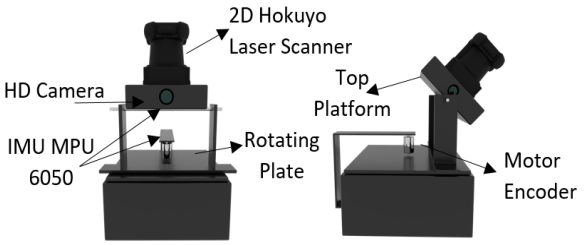

(a) (b)

Fig. 4. 3D CAD model of scanning system: (a) front and (b) side views.

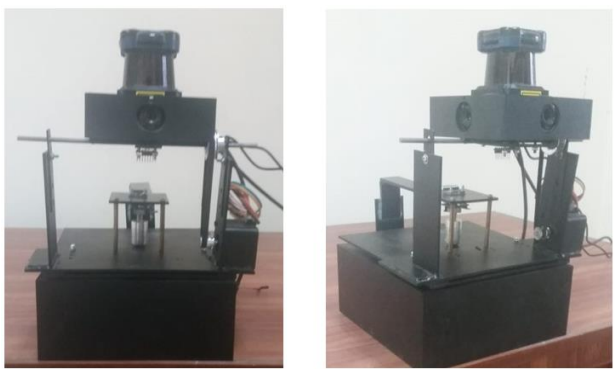

Fig. 5. Multiple views of the actual 3D scanning system.

B. Instrumentation Design

The instrumentation scheme of the stationary scanning system is shown in Fig. 6.

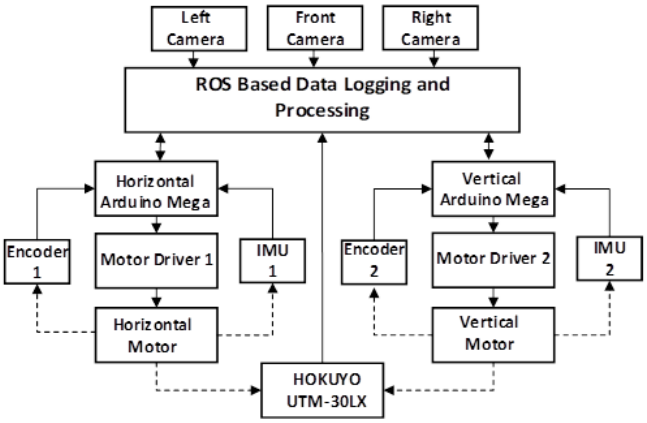

Fig. 6. Instrumentation design for online operation of the scanning system.

The system comprises of two motorised platforms that can rotate in horizontal and vertical directions. Each stepper motor has been controlled by Arduino mega controller board, and the rotational rate feedback of the motor has been provided by encoder to Arduino board. The angular displacement feedbacks have been provided by both IMUs to respective controller boards which deliver ON-OFF control commands to the designated motor drivers. Both controllers have been connected through USB ports to the laptop having Robot Operating System (ROS). The desired rotational rates for the platforms have been sent serially by the laptop to the controllers. The controllers have implemented the commands and sent back the continuous rotational feedbacks to the laptop to generate the 3D point cloud of the vicinity. The rotating speed is kept low to scan properly. The laser scanner has been connected to the network port of the laptop, while three HD cameras have been interfaced to ROS through USB ports. All the online data have been viewed in RVIZ package of ROS and stored in a ROS bag file for offline processing using Matlab scripting as shown in Fig. 7. The stored scans, encoders, and IMU data have been filtered and processed for 3D registration of scan points to build the 3D point cloud. Later, the segmentation of geometrical planes have been performed on developed point cloud to view the structural details of the vicinity. Finally, the BIM of the surveyed region with 2D floor plan has been made.

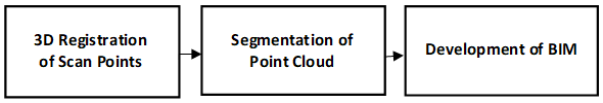

Fig. 7. Implementation steps for offline operation.

The scanning spaces of a single 2D Hokuyo laser scanner and the developed stationary scanning system are shown in Fig. 8. The single scanner has a limited 2D view of the region, while the developed two degree of freedom (DOF) motorised scanning system has the complete 3D spherical scanning space of radius 30 m. The individual horizontal and vertical motorised scanning lines are shown in blue and red colours, respectively, which can perceive the environment thoroughly according to the assigned rotational

values generating by the controlling boards of the scanning system.

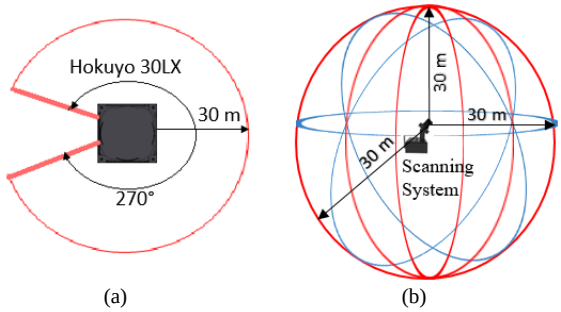

(a) (b)

Fig. 8. Scanning spaces: (a) single scanner and (b) the developed system.

Scanning spaces of single motorised 3D scanning platforms have been presented in recent research works [20], [21]. However, the appearance of dead zones cannot be eliminated until an additional motorised joint is included as proposed in this research work. Furthermore, some important characteristics of the developed scanning system have been summarised in Table II in comparison to the properties of two compact 3D laser scanners, SICK MRS1000P and Velodyne PUCK scanners [22], [23]. The scanning spaces of both 3D scanners are shown in Fig. 9. The SICK scanner has a limited horizontal field of view (FOV) while Velodyne offers complete circular horizontal FOV.

TABLE II. COMPARISON OF DEVELOPED 3D LASER SCANNING SYSTEM.

Parameter	SICK MRS1000P	Velodyne PUCK	Developed System
Maximum Range (m)	60	100	30
Horizontal FOV (deg.)	270	360	360
Vertical FOV (deg.)	7.5	30	180
Cost ($)	7600	31,200	4500

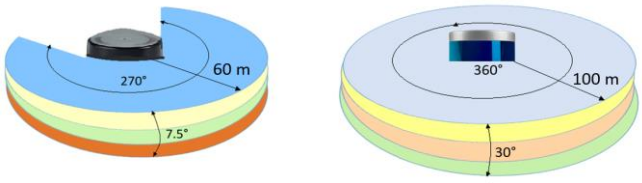

(a) (b)

Fig. 9. Scanning spaces of scanners: (a) SICK MRS and (b) Velodyne.

The measuring ranges, data points, and sampling rate of both scanners have better values than the developed system. However, both 3D scanners have narrowed vertical FOV due to which they can only scan the environment partially in stationary conditions and will need additional movements to cover the default gap of FOVs. According to surveyor requirements, the developed system has the ability to scan with greater vertical FOV to provide more enhanced perception of the vicinity in a single go at a highly affordable cost compared to other peers as shown in Table II [24].

IV. 3D POINT CLOUD GENERATION AND BIM DEVELOPMENT

The generation scheme of 3D point cloud and its building information modelling have been presented in this section. Figure 10(a) shows the conceptual working of the scanner, which can rotate horizontally and vertically through motors according to the commands shown by the green and cyan arrows. Figure 10(b) indicates the scan line falling on multiple planes in front of the scanner. The up and down movements of the scan line can be controlled as per given rotational commands to the motors, which may ultimately be used to completely scan the environment.

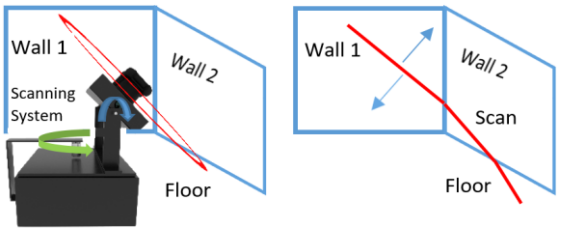

(a) (b)

Fig. 10. (a) Scanning operation; (b) Scan line perceiving many planes.

The methodology for getting 3D Cartesian points using 2D laser scanning of the surveyed environment involves at its core an accurate adaptation of transformation scheme suitable for such kinds of stationary scanning systems. The developed scanning system has been considered similar to an industrial manipulator of two joints and two links as shown in Fig. 11. To establish transformation representation for this system, a popular Denavit-Hartenburg (DH) parameterisation scheme has been used [25].

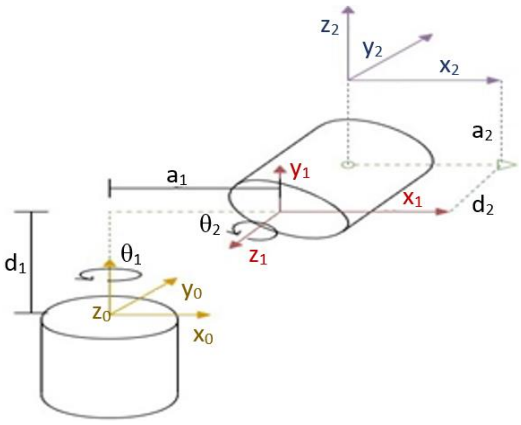

Fig. 11. Scanning system representation in terms of joints and links.

The first and second joints of the system with local frames $X_0Y_0Z_0$ and $X_1Y_1Z_1$ indicate motorised rotations of the base and top plates by θ_1 and θ_2, respectively. The first link with the translational displacements of (a_1, 0, d_1) indicates the placement of the top plate with respect to the base plate. The second link with the translational displacements of (0, a_2, d_2) indicates the placement of the 2D laser scanner with respect to top plate. According to the DH parameterisation scheme, the transformation equation from the first to the second joint can be written as shown in (1)

$$\mathbf{A_1} = \mathbf{Rot}(z,\theta_1)\times\mathbf{Trans}(0,0,d_1)\times \\ \times\mathbf{Trans}(a_1,0,0)\times\mathbf{Rot}(x,-90^{\circ}). \quad (1)$$

The resultant matrix A_1 generated after multiplication of individual rotational and translational matrices can be written as shown in (2)

$$\mathbf{A_1}=\begin{bmatrix}\cos(\theta_1) & -\sin(\theta_1)\cos(90^\circ) & -\sin(\theta_1)\sin(90^\circ) & a_1\cos(\theta_1)\\ \sin(\theta_1) & \cos(\theta_1)\cos(90^\circ) & \cos(\theta_1)\sin(90^\circ) & a_1\sin(\theta_1)\\ 0 & -\sin(90^\circ) & \cos(90^\circ) & d_1\\ 0 & 0 & 0 & 1\end{bmatrix}. \quad (2)$$

The second link ending in scanner's local frame $X_2Y_2Z_2$ has translational displacements of (a_2, d_2) in the Y_1Z_1 plane of the second joint and eventually will change the values in the respective translational matrices. By keeping the given DH parametric order of multiplication, the overall transformation equation from the second joint can be shown in (3)

$$\mathbf{A_2}=\mathbf{Rot}(z,\theta_2)\times\mathbf{Trans}(0,0,d_2)\times \\ \times\mathbf{Trans}(0,a_2,0)\times\mathbf{Rot}(x,90^\circ). \quad (3)$$

The system design has been made in such a way that the displacement d_2 holds a minute value so that the resultant matrix A_2 can be written as shown in (4)

$$\mathbf{A_2}=\begin{bmatrix}\cos(\theta_2) & -\sin(\theta_2)\cos(90^\circ) & \sin(\theta_2)\sin(90^\circ) & -a_2\sin(\theta_2)\\ \sin(\theta_2) & \cos(\theta_2)\cos(90^\circ) & -\cos(\theta_2)\sin(90^\circ) & a_2\cos(\theta_2)\\ 0 & \sin(90^\circ) & \cos(90^\circ) & d_2\\ 0 & 0 & 0 & 1\end{bmatrix}. \quad (4)$$

Therefore, the complete transformation T_C of the scanning system, including all joints and links, can be shown in (5)

$$\mathbf{T_C}=\mathbf{A_1}\times\mathbf{A_2}. \quad (5)$$

Now using the distinct 2D Cartesian point P_S of each recorded scan at the respective time stamp, the transformation of the point into a 3D Cartesian coordinate point P_T can be achieved as shown in (6)

$$\mathbf{P_T}=\mathbf{T_C}\times\mathbf{P_S}. \quad (6)$$

When repeating the transformation step for all the scan points belonging to any particular scan, the complete scan can be registered into a global 3D coordinated frame. The similar mechanism can be prolonged for all recorded scans, and all the generated points can be accumulated to form the complete 3D point cloud of the surveying region. The overall implementation has been performed in MATLAB coding. When considering possible manufacturing defects in the scanning system, the acceptable accuracy in the point cloud cannot be achieved. These defects may occur in any mechanical design parameters of d_1, a_1, d_2, and a_2 as shown in Fig. 12 by red colours. Due to these defects, actually incorrect values will be processed in the presented point cloud development scheme. Therefore, more realistic values have been required expressing the actual dimensions of the setup to achieve the most accurate mapping results.

Let us include the possibilities of errors in the d_1 and a_1 design parameters as shown in (7)

$$\mathbf{A_{1e}}=\mathbf{Rot}(z,\theta_1)\times\mathbf{Trans}(0,0,d_1+\varepsilon_1)\times \\ \times\mathbf{Trans}(a_1+\varepsilon_2,0,0)\times\mathbf{Rot}(x,-90^\circ). \quad (7)$$

Similarly, let us include the possibilities of errors in the d_2 and a_2 design parameters as shown in (8)

$$\mathbf{A_{2e}}=\mathbf{Rot}(z,\theta_2)\times\mathbf{Trans}(0,0,d_2+\varepsilon_3)\times \\ \times\mathbf{Trans}(0,a_2+\varepsilon_4,0)\times\mathbf{Rot}(x,90^\circ). \quad (8)$$

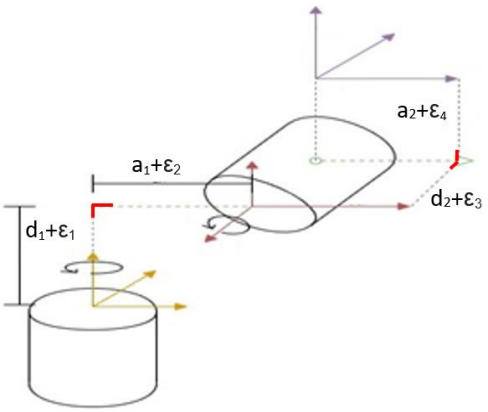

Fig. 12. Possible mechanical defects appearing in the design parameters.

Each possible defect, say $\mathcal{E}_1$ has a given bipolar error range provided by the manufacturer. Taking a set of initial possible values for all errors, using (7) and (8), a point cloud of a smooth wall plane has been developed fulfilling the standard plane equation $n_p.X_{sp} = -d_p$, where n_p is the normal vector, d_p is the distance of the wall plane from the origin, and X_{SP} is the relevant scanned point. Due to the presence of errors, not all scanned points can satisfy the developed plane model, so placing the first scanned point in the developed equation to determine its absolute plane fitting error $\mathcal{E}_{n1}$ as shown in (9)

$$\varepsilon_{n1}=\left|n_p.X_{sp}+d_p\right|. \quad (9)$$

Placing all scanned points in the same manner, all error terms have been used to determine the standard deviation of the errors R_q or the root mean square error (*RMSE*) using (10) [26]

$$R_q=\left[\left(\sum_{i=1}^{N}\varepsilon_{ni}^2\right)/N\right]^{1/2}. \quad (10)$$

Repeating the same calculation of R_q for all possible sets of errors has provided the most appropriate set of mechanical parameters where the respective R_q has been found minimum. Using these parameters, the scanning system has been tested in various vicinities. The first testing has been carried out in an indoor lab region as shown in Fig. 13.

The scanning system has been placed at *A, B, and C* locations inside the indoor lab as shown in Fig. 14. At each place, the scanning system has recorded many scans varying θ_1 and θ_2 from -90 ° to +90 °, respectively. Distinct point clouds have been developed at each location containing precise 3D scan points of the portion of the vicinity around that placement.

Fig. 13. Scanning of an indoor region using the stationary system.

Finally, all individual point clouds have been merged using the parallel translational values present among different placements as shown below.

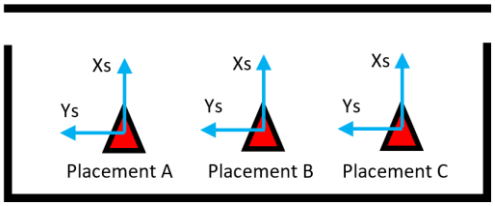

Fig. 14. Placement of the scanning system at parallel locations.

The complete point cloud of the lab is shown in Fig. 15(a). Using the MATLAB implementation of the Random Sample Consensus (RANSAC) algorithm, the point cloud has been segmented into various structural planes [27]. By removing the ceiling, side walls and floor planes, inside view of the lab are shown in Fig. 15(b). Multiple furniture items, front walls, and some pillars are visible. Still some portions have not been scanned and can be viewed if more placements may be used to record additional scans.

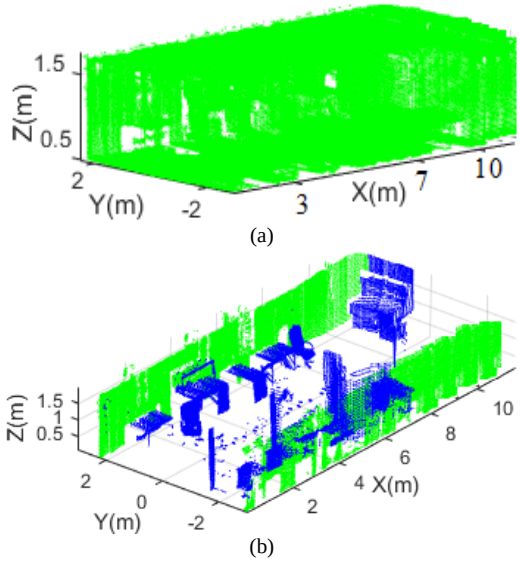

Fig. 15. (a) Developed point cloud of the indoor region; (b) Inside view of the lab by removing the ceiling and floor planes.

The generated point cloud has been used to make a BIM of the surveyed vicinity using popular Autodesk REVIT BIM software as shown in Fig. 16 [28]. The wall boundaries have been developed in REVIT using point cloud, and then window objects have been placed. Small manual assistance has been performed on point windows or pillars correctly because some objects were not clearly visible during the scanning. The overall BIM development of the floor plan has taken small time at affordable rate, and additionally the result has been verified with ground truth of the region.

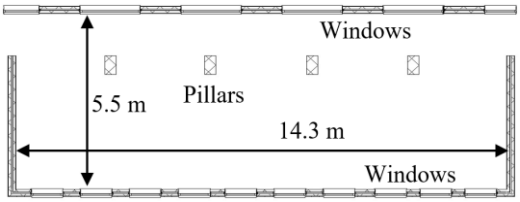

Fig. 16. The developed BIM floor plan of the indoor lab.

The complete 3D BIM of the surveyed vicinity is shown in Fig. 17.

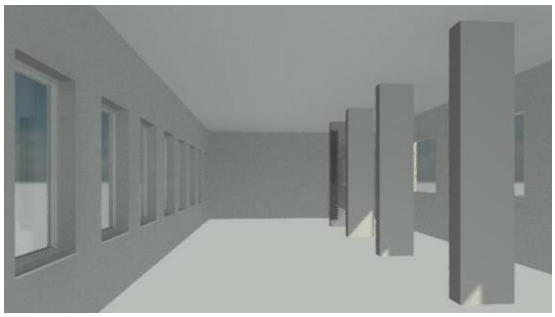

Fig. 17. The complete 3D BIM developed of the indoor lab.

All the structural entities are clearly visible and measurable as required by the building contractors and surveyors for doing renovation and other related tasks. Therefore, the overall procedure for scanning to BIM development has been performed economically.

V. RESULTS

The stationary scanning system has been tested in multiple regions. Figure 18 shows the usage of the system in a corridor environment. The scanning system has been placed at various parallel locations inside the corridor just like in the case explained for the indoor lab scanning test.

Fig. 18. Scanning of a corridor region using the stationary scanning system.

At each placement, the scanning system has recorded multiple scans by varying θ_1 and θ_2 and later by merging, the complete point cloud is shown in Fig. 19.

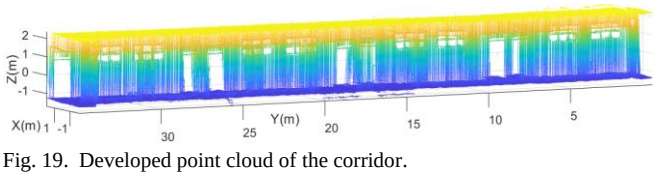

Fig. 19. Developed point cloud of the corridor.

The generated point cloud represents structural details of the corridor very clearly. The point cloud has been loaded in REVIT and its 3D view is shown in Fig. 20(a), while an inside view of the corridor is shown in Fig. 20(b).

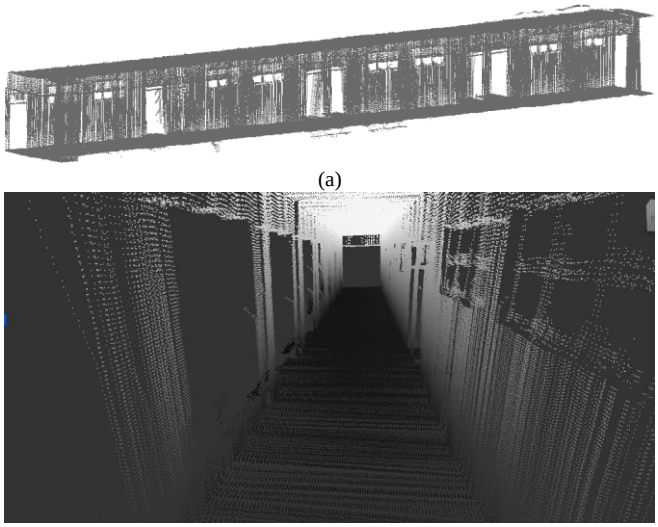

(a)

(b)

Fig. 20. (a) Complete view of the developed point cloud in REVIT; (b) An inside view of the developed point cloud in REVIT.

The structural details, windows, doors, and open spaces, are visible on the left and right side of the Fig. 20(b), respectively. Later the point cloud is used for making the BIM and the floor plan of the surveyed vicinity with little human assistance specifically for some objects which were partially scanned. The result of the floor plan is shown in Fig. 21 and verified with the ground truth as compared in Table III.

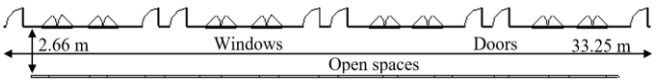

Fig. 21. The developed BIM floor plan of the corridor.

TABLE III. COMPARISON OF MEASURED RESULTS.

Experiment	Corridor		Outdoor region	
	Actual	Measured	Actual	Measured
Length (m)	33.5	33.25	30	29.7
Width (m)	2.65	2.66	20	19.9

The complete 3D BIM of the corridor vicinity is shown in Fig. 22. The wall, floor, and ceiling objects have been made first by following the traces of loaded point cloud. Later, the windows, doors, and open spaces have been marked inside the BIM. All the structural details are clearly observable in the developed model and can be further used to quantify the specific region for the newly assigned construction job. The overall labour work has been drastically reduced through stationary scanning and it took quite a while to complete the job at affordable rates.

The stationary scanning system has been tested in an outdoor region near the athletic track as shown in Fig. 23. The track is surrounded by a large concrete slope, trees, and vegetation. That was the most challenging environment to scan as the surveying vicinity had no regular geometrical structures and most of the view was open and could not be scanned. Even the ground plane was uneven to properly place the system. After some careful settings with the system, the scanning job was carried out.

Fig. 22. The BIM developed for the corridor.

Fig. 23. Scanning of an outdoor region near an athletic track.

The stationary system has been placed at two different parallel locations to scan the region. At each placement, the scanning system has recorded distinct point clouds, and later both have merged to generate the complete point cloud of the region as shown in Fig. 24. The development of outdoor point cloud has appeared comparatively easy and did not require computationally expensive algorithms and hardware such as SLAM mapping techniques running on some moving scanning systems.

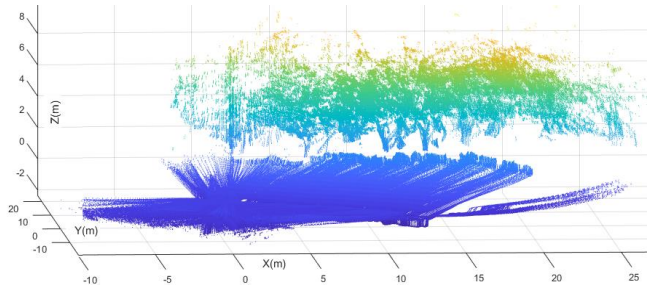

Fig. 24. Developed point cloud of the outdoor region.

The generated point cloud represents structural details along with the mapping of trees and plantation present in the outdoor vicinity. Figure 25 shows the view of the developed point cloud inside the REVIT software. There are very few regular structures present in the point cloud, including the floor plane and the concrete slope. Therefore, a quite small modelling task has been performed by tracing the loaded point cloud. Furthermore, the appearance of trees and

nearby plantation was very challenging to discriminate with each other, certainly requiring extra testing and fitting of the respective details along with human assistance in the development of BIM.

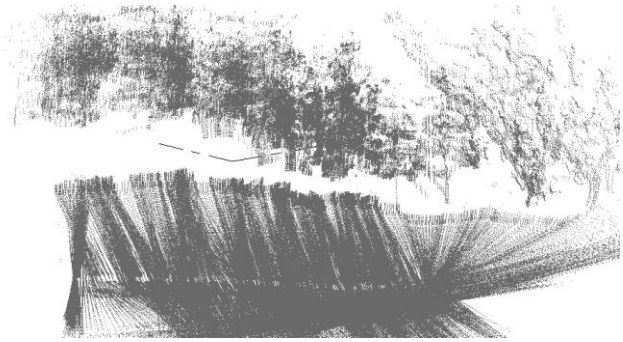

Fig. 25. View of the developed point cloud in REVIT.

The generated 3D BIM result is shown in Fig. 26.

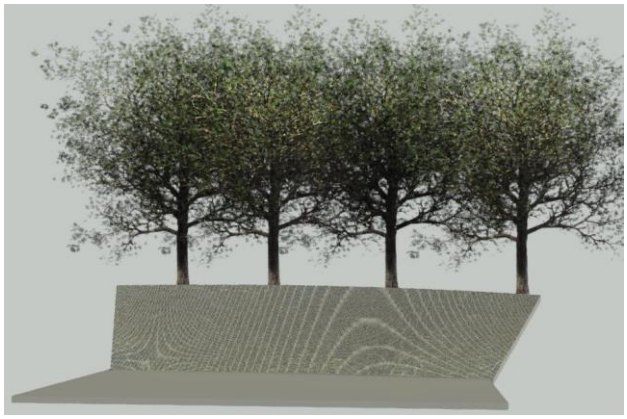

Fig. 26. The developed BIM of the outdoor vicinity.

The floor and slope objects have been created as observed by the scanned points. The generated dimensions have been verified with ground truth of the region and found to be 98 % accurate as shown in Table III. In addition, the tree objects were added in the BIM as observed in the point cloud. However, placing a similar tree pattern along with the demarcation between them appeared quite challenging tasks and partially resolved with manual assistance.

VI. CONCLUSIONS

This research work presents the operation of the indigenously developed economical stationary survey and scanning system. The generated 3D mapping results of the system have been found to be 96 % accurate if compared with the actual dimensions of the surveyed vicinities. The total time consumed for generating the surveying results has been minimized to 40 % with ease of operation if compared to the available surveying techniques in the regional market. In addition, the development of BIM for floor plans and 3D elevations model has been shown, which is a very useful requirement for surveyors and civil contractors. Overall system handling and operation has been found to be fairly simple and easy to train the surveyors to do digital scanning. To further improve the localization and visualization of the surveyed regions, the recorded monocular vision information will be used in future work with the latest classification and segmentation techniques.

ACKNOWLEDGMENT

The authors thank the staff of the Department of Electronic Engineering, NEDUET, for their continuous help and support.

CONFLICTS OF INTEREST

The authors declare that they have no conflicts of interest.

REFERENCES

[1] G. Lenda, A. Uznanski, M. Strach, and P. Lewinska, “Laser scanning in engineering surveying: Methods of measurement and modeling of structures”, *Reports on Geodesy and Geoinformatics*, vol. 100, no. 1, pp. 109–130, 2016. DOI: 10.1515/rgg-2016-0010.

[2] A. Keitaanniemi, J.-P. Virtanen, P. Rönnholm, A. Kukko, T. Rantanen, and M. T. Vaaja, “The combined use of SLAM laser scanning and TLS for the 3D indoor mapping”, *Buildings*, vol. 11, no. 9, p. 386, 2021. DOI: 10.3390/buildings11090386.

[3] L. Klingbeil, C. Eling, E. Heinz, and M. Wieland, “Direct georeferencing for portable mapping systems: In the air and on the ground”, *Journal of Surveying Engineering*, vol. 143, no. 4, Nov. 2017. DOI: 10.1061/(ASCE)SU.1943-5428.0000229.

[4] E. Nocerino, F. Menna, F. Remondino, I. Toschi, and P. Rodríguez-Gonzálvez, “Investigation of indoor and outdoor performance of two portable mobile mapping systems”, in *Proc. of Conference Videometrics, Range Imaging and Applications XIV*, 2017, pp. 125–139, vol. 10332. DOI: 10.1117/12.2270761.

[5] U. Stenz, J. Hartmann, J.-A. Paffenholz, and I. Neumann, “High precision 3D object capturing with static and kinematic terrestrial laser scanning in industrial applications, approaches of quality assessment”, *Remote Sensing*, vol. 12, no. 2, p. 290, 2020. DOI: 10.3390/rs12020290.

[6] J. Morales, V. Plaza-Leiva, A. Mandow, J. A. Gomez-Ruiz, J. Seron, and A. Garcia-Cerezo, “Analysis of 3D scan measurement distribution with application to a multi-beam lidar on a rotating platform”, *Sensors*, vol. 18, no. 2, p. 395, 2018. DOI: 10.3390/s18020395.

[7] Y.-S. Chou and J.-S. Liu, “A robotic indoor 3D mapping system using a 2D laser range finder mounted on a rotating four-bar linkage of a mobile platform”, *International Journal of Advanced Robotic Systems*, vol. 10, 2013. DOI: 10.5772/54655.

[8] “ZEB Go Handheld 3D Scanner: Laser Scanning for Everyone”, *GeoSLAM*. [Online]. Available: https://geoslam.com/solutions/zeb-go/

[9] “ZEB Revo RT: Handheld Laser Point Cloud Scanner”, *GeoSLAM*. [Online]. Available: https://geoslam.com/solutions/zeb-revo-rt/

[10] “ZEB Horizon: SLAM LiDAR for 3D Mapping with Drones”, *GeoSLAM*. [Online]. Available: https://geoslam.com/solutions/zeb-horizon/

[11] C. Stal, J. Verbeurgt, L. De Sloover, and A. De Wulf, “Assessment of handheld mobile terrestrial laser scanning for estimating tree parameters”, *Journal of Forestry Research*, vol. 32, pp. 1503–1513, 2021. DOI: 10.1007/s11676-020-01214-7.

[12] K. L. Chow, “Engineering survey applications of terrestrial laser scanner in highways department of the government of Hong Kong Special Administration Region (HKSAR)”, in *Proc. of Strategic FIG Working Week: Integration of Surveying Services*, 2007.

[13] “Leica ScanStation P50 - Long Range 3D Terrestrial Laser Scanner”, Leica Geosystems. [Online]. Available: https://leica-geosystems.com/products/laser-scanners/scanners/leica-scanstation-p50

[14] “FARO Focus Laser Scanners”, FARO. [Online]. Available: https://www.faro.com/en/Products/Hardware/Focus-Laser-Scanners

[15] “RIEGL Laser Measurement Systems”. [Online]. Available: http://www.riegl.com/uploads/tx_pxpriegldownloads/RIEGL_VZ-2000i_Infosheet_2019-09-02.pdf

[16] L. Kurnianggoro, V.-D. Hoang, and K.-H. Jo, “Calibration of a 2D laser scanner system and rotating platform using a point-plane constraint”, *Computer Science and Information Systems*, vol. 12, pp. 307–322, 2015. DOI: 10.2298/CSIS141020093K.

[17] Z. Fang, S. Zhao, S. Wen, and Y. Zhang, “A real-time 3D perception and reconstruction system based on a 2D laser scanner”, *Journal of Sensors*, vol. 2018, 2018. DOI: 10.1155/2018/2937694.

[18] M. G. Ocando, N. Certad, S. Alvarado, and Á. Terrones, “Autonomous 2D SLAM and 3D mapping of an environment using a single 2D LIDAR and ROS”, in *Proc. of 2017 Latin American Robotics Symposium (LARS) and 2017 Brazilian Symposium on*

Robotics (SBR), 2017, pp. 1–6. DOI: 10.1109/SBR-LARS-R.2017.8215333.

[19] M. Bosse and R. Zlot, "Continuous 3D scan-matching with a spinning 2D laser", in *Proc. of 2009 IEEE International Conference on Robotics and Automation*, 2009, pp. 4312–4319. DOI: 10.1109/ROBOT.2009.5152851.

[20] S. Schubert, P. Neubert, and P. Protzel, "How to build and customize a high resolution 3D laser scanner using off the shelf components", in *Towards Autonomous Robotic Systems. TAROS 2016. Lecture Notes in Computer Science()*, vol. 9716. Springer, Cham, 2016, pp. 314–326. DOI: 10.1007/978-3-319-40379-3_33.

[21] S. Bi, C. Yuan, C. Liu, J. Cheng, W. Wang, and Y. Cai, "A survey of low-cost 3D laser scanning technology", *Applied Sciences*, vol. 11, no. 9, p. 3938, 2021. DOI: 10.3390/app11093938.

[22] 3D SICK Laser Scanner MRS1000P. [Online]. Available: https://www.sick.com/ag/en/detection-and-ranging-solutions/3d-lidar-sensors/mrs1000/c/g387152

[23] 3D Velodyne Puck Laser Scanner, Velodyne Lidar. [Online]. Available: https://velodynelidar.com/products/puck/

[24] Chironix product search: SICK MRS1000. [Online]. Available: https://www.chironix.com/sensors-accessories/sick-mrs1000-outdoor

[25] J. Denavit and R. S. Hartenberg, "A kinematic notation for lower-pair mechanisms based on matrices", *Journal of Applied Mechanics*, vol. 22, no. 2, pp. 215–221, 1955. DOI: 10.1115/1.4011045.

[26] S. Gerbino, D. M. Del Giudice, G. Staiano, A. Lanzotti, and M. Martorelli, "On the influence of scanning factors on the laser scanner-based 3D inspection process", *The International Journal of Advanced Manufacturing Technology*, vol. 84, pp. 1787–1799, 2016. DOI: 10.1007/s00170-015-7830-7.

[27] M. A. Fischler and R. C. Bolles, "Random sample consensus: A paradigm for model fitting with applications to image analysis and automated cartography", *Communications of the ACM*, vol. 24, no. 6, pp. 381–395, 1981. DOI: 10.1145/358669.358692.

[28] R. Laing, M. Leon, J. Isaacs, and D. Georgiev, "Scan to BIM: The development of a clear workflow for the incorporation of point clouds within a BIM environment", *WIT Transactions on the Built Environment*, vol. 149, pp. 279–289, 2015. DOI: 10.2495/BIM150241.